Reflecting boundary conditions for interferometry by multidimensional deconvolution

Cornelis Weemstra, Kees Wapenaar and Karel N. van Dalen, Delft University of Technology*

SUMMARY

In this work we investigate a modification of the formulation of the theory underlying seismic interferometry (SI) by multidimensional deconvolution (MDD). The current formulation, and hence method, relies on separation of waves traveling inward and outward of a volume bounded by receivers. As a consequence, it is predominantly useful when receivers are illuminated from one side only. This puts constraints on the applicability of SI by MDD to omnidirectional wave fields. The proposed modification eliminates the requirement to separate inward-and outward propagating wave field and, consequently, improves the applicability of MDD to omnidirectional wave fields. We therefore envisage the modified MDD formulation to hold significant promise in the application to ambient-noise surface wave data.

INTRODUCTION

Seismic interferometry (SI) refers to the principle of generating new seismic responses from existing recordings. A virtual source response can be obtained by simple crosscorrelation of seismic observations at two receiver locations (Bakulin and Calvert, 2004). In case of controlled sources, the process involves an additional summation of crosscorrelations over different source positions (e.g., Froment et al., 2010). Applied to passive wave fields, no explicit summation over source locations is required, because the simultaneously acting sources are uncorrelated. Obtaining the virtual source response by means of simple crosscorrelations will be referred to as "SI by crosscorrelation" in this paper.

Responses obtained by SI by crosscorrelation can be related to the Green's function of the medium under specific conditions: the medium is required to be lossless and needs to be illuminated with equal power from all directions (Wapenaar and Fokkema, 2006). Reformulating the theory underlying SI by crosscorrelation in terms of a multidimensional deconvolution (MDD) process relaxes these conditions (Wapenaar and van der Neut, 2010; Wapenaar et al., 2011). Most notably, multidimensional deconvolution acknowledges the 3D nature of the wave field, i.e., MDD corrects for non-uniformities in the illumination pattern. We will refer to the multidimensional deconvolution process as "SI by MDD" in the remainder of this work.

ACOUSTIC REPRESENTATION THEOREM

Consider the configuration shown in Figure 1 where a volume $\mathbb{V}$ is bounded by a surface $\mathbb{S}$ with outward pointing normal vector $\mathbf{n}$. We define a reference Green's function $\bar{G}_R \equiv \bar{G}(\mathbf{x}_R, \mathbf{x}, t)$, which gives the pressure at $\mathbf{x}_R$ due to an impulsive point source of volume injection rate at $\mathbf{x}$ (Wapenaar and Fokkema, 2006). Similarly, we define a Green's function $G_S \equiv G(\mathbf{x}, \mathbf{x}_S, t)$, which gives the pressure at $\mathbf{x}$ due to an impulsive point source of volume injection rate at $\mathbf{x}_S$. Moreover, we prescribe $\mathbf{x}_S$ to be situated outside $\mathbb{S}$, whereas we choose $\mathbf{x}_R$ inside $\mathbb{S}$. The reference Green's function $\bar{G}_R$ is associated with a reference medium and/or boundary conditions (hence the bar), whereas G_S is associated with the actual medium. Assuming identical medium parameters for $\bar{G}_R$ and G_S inside $\mathbb{S}$, but a different reference medium outside of $\mathbb{S}$, a convolution-type representation for the Green's function can be derived (Wapenaar and van der Neut, 2010),

$$G(\mathbf{x}_R, \mathbf{x}_S, t) = \int_{\mathbb{S}} \frac{1}{i\omega\rho(\mathbf{x})} \left(\bar{G}_R * \nabla G_S - G_S * \nabla \bar{G}_R\right) \cdot \mathbf{n}\, d\mathbf{x}. \quad (1)$$

The spatial derivatives are computed on $\mathbb{S}$, i.e., at $\mathbf{x}$, and the in-line asterisk $*$ denotes temporal convolution. Angular frequency, mass density and imaginary unit are given by ω, ρ and i, respectively. Note that $[-i\omega\rho(\mathbf{x})]^{-1} \nabla G_S \cdot \mathbf{n}$ represents the particle velocity at $\mathbf{x}$ perpendicular to $\mathbb{S}$, whereas $[i\omega\rho(\mathbf{x})]^{-1} \mathbf{n} \cdot \nabla \bar{G}_R$ represents the response at $\mathbf{x}_R$ due to a dipole source at $\mathbf{x}$. The medium in $\mathbb{V}$ can be arbitrary heterogeneous and equation 1 holds for media with losses. While G_S and $G(\mathbf{x}_R, \mathbf{x}_S, t)$ are related to the observed wave field, the reference Green's function $\bar{G}_R$ is not. This allows us to choose convenient boundary conditions for $\bar{G}_R$ at $\mathbb{S}$.

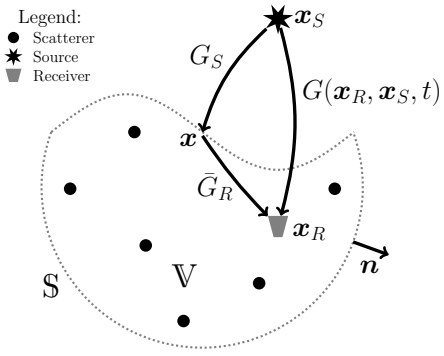

Figure 1: *Configuration for the convolution-type Greens function representation (eq. 1). The rays associated with G_S and $G(\mathbf{x}_R, \mathbf{x}_S, t)$ represent full responses, including scattered arrivals due to inhomogeneities inside as well as outside $\mathbb{S}$. The reference Green's function $\bar{G}_R$ represents the full response of the medium in $\mathbb{V}$ plus possible additional effects associated with the choice of the boundary conditions at $\mathbb{S}$ and/or different medium parameters outside $\mathbb{S}$.*

Absorbing boundary conditions

Conventionally, the integrand in eq. 1 is simplified assuming absorbing boundary conditions along $\mathbb{S}$ for $\bar{G}_R$. This implies that its reciprocal $\bar{G}(\mathbf{x}, \mathbf{x}_R, t)$ is outward propagating at $\mathbf{x}$ on $\mathbb{S}$. Additionally writing G_S as a superposition of inward and outward propagating fields at $\mathbf{x}$ on $\mathbb{S}$, assuming $\mathbb{S}$ to be sufficiently

smooth, and assuming ρ constant along $\mathbb{S}$, eq. 1 simplifies to (Wapenaar et al., 2011),

$$G(\mathbf{x}_R,\mathbf{x}_S,t) = 2\int_{\mathbb{S}_{rec}} \bar{G}_R^{(d)}(\mathbf{x}_R,\mathbf{x},t) * G_S^{(in)}(\mathbf{x},\mathbf{x}_S,t)\; d\mathbf{x}. \qquad (2)$$

The superscript (d) denotes that $\bar{G}_R^{(d)}$ is a dipole Green's function: $\bar{G}_R^{(d)} \equiv [-i\omega\rho]^{-1}\,\mathbf{n}\cdot\nabla\bar{G}_R$. In many practical situations the wave field is not recorded along a closed boundary, which necessarily limits the integration surface to an open receiver boundary. We have therefore replaced $\mathbb{S}$ with $\mathbb{S}_{rec}$ where the subscript 'rec' refers to that part of $\mathbb{S}$ on which G_S is available. Integration along $\mathbb{S}_{rec}$ suffices in case sources only exist on the appropriate side of $\mathbb{S}_{rec}$: radiation conditions apply over the half sphere $\mathbb{S}_0$ that closes $\mathbb{S}$. The integral along $\mathbb{S}_0$ therefore evaluates to zero. Figure 2a shows an example of a configuration with an open receiver boundary $\mathbb{S}_{rec}$.

To comply with practice, the Green's functions related to the observed wave field are convolved with a (transient) source function $s(\mathbf{x}_S,t)$, yielding,

$$p(\mathbf{x}_R,\mathbf{x}_S,t) = 2\int_{\mathbb{S}_{rec}} \bar{G}_R^{(d)}(\mathbf{x}_R,\mathbf{x},t) * p^{(in)}(\mathbf{x},\mathbf{x}_S,t)\; d\mathbf{x}, \qquad (3)$$

where $p(\mathbf{x}_R,\mathbf{x}_S,t) \equiv G(\mathbf{x}_R,\mathbf{x}_S,t) * s(\mathbf{x}_S,t)$ and $p^{(in)}(\mathbf{x},\mathbf{x}_S,t) \equiv G_S^{(in)}(\mathbf{x},\mathbf{x}_S,t) * s(\mathbf{x}_S,t)$. Assuming a multitude of sources exist (on the appropriate side of $\mathbb{S}_{rec}$), eq. (3) can be solved in a least-square sense (Wapenaar and van der Neut, 2010). The normal equation is obtained by crosscorrelating both sides with the $p^{(in)}\left(\mathbf{x}',\mathbf{x}_S^{(k)},t\right)$ (pressure at $\mathbf{x}'$ due to source number k at source position $\mathbf{x}_S^{(k)}$):

$$C\left(\mathbf{x}_R,\mathbf{x}',t\right) = 2\int_{\mathbb{S}_{rec}} \bar{G}_R^{(d)}(\mathbf{x}_R,\mathbf{x},t) * \Gamma\left(\mathbf{x},\mathbf{x}',t\right)\; d\mathbf{x}, \qquad (4)$$

where

$$C\left(\mathbf{x}_R,\mathbf{x}',t\right) \equiv \sum_k p\left(\mathbf{x}_R,\mathbf{x}_S^{(k)},t\right) * p^{(in)}\left(\mathbf{x}',\mathbf{x}_S^{(k)},-t\right) \qquad (5)$$

and,

$$\Gamma\left(\mathbf{x},\mathbf{x}',t\right) \equiv \sum_k p^{(in)}\left(\mathbf{x},\mathbf{x}_S^{(k)},t\right) * p^{(in)}\left(\mathbf{x}',\mathbf{x}_S^{(k)},-t\right) \qquad (6)$$

Equation (4) shows how crosscorrelation function $C(\mathbf{x}_R,\mathbf{x}',t)$ is proportional to the sought for dipole Green's function $\bar{G}_R^{(d)}$ smeared in space and time by the point-spread function $\Gamma(\mathbf{x},\mathbf{x}',t)$. If the sources do not illuminate $\mathbb{S}_{ref}$ uniformly, the distortion of $C(\mathbf{x}_R,\mathbf{x}',t)$ with respect to $\bar{G}_R^{(d)}$ is quantified by the point-spread function. SI by MDD encompasses deconvolving the correlation function for the point-spread function. For details regarding the inversion, we refer to van der Neut (2012). Minato et al. (2011) and Poletto and Bellezza (2012) report successful inversion for $\bar{G}_R^{(d)}$ using crosswell seismic reflection data and reflection data in an arctic environment, respectively.

Often waves propagate inward to as well as outward from $\mathbb{V}$. Separation of these inward-and outward propagating fields is then required. Wave field separation, either in time or space, however, relies on assumptions that are often not fully satisfied. It may therefore be more appropriate to assume a reflecting boundary for $\bar{G}_R$.

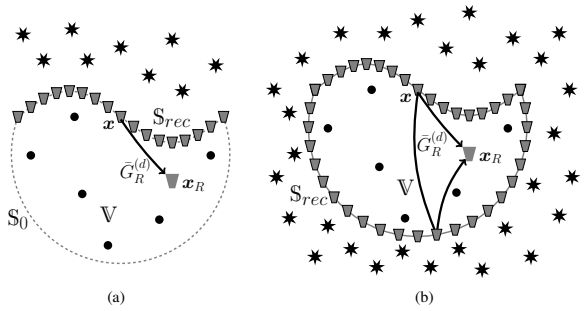

Figure 2: *Configurations associated with an absorbing boundary (a) and a reflecting boundary (b). The retrieved Green's function $\bar{G}_R^{(d)}$ in (b) includes 'reflections' from the receiver boundary.*

Reflecting boundary conditions

We now consider the pressure to be zero on $\mathbb{S}_{rec}$ in the reference medium, i.e., $\bar{G}_R = 0$ (note that this also implies that the particle velocity tangent to $\mathbb{S}_{rec}$ vanishes). In this situation eq. 1 simplifies to,

$$G(\mathbf{x}_R,\mathbf{x}_S,t) = \int_{\mathbb{S}_{rec}} \bar{G}_R^{(d)}(\mathbf{x}_R,\mathbf{x},t) * G_S(\mathbf{x},\mathbf{x}_S,t)\; d\mathbf{x}. \qquad (7)$$

This equation has two notable differences with respect to eq. 2. First, instead of the inward propagating wave field on $\mathbb{S}_{rec}$, the full wave field is considered. Second, the right-hand side of eq. 7 lacks a factor two. Physically, the absence of this factor can be explained by the reflecting nature of $\mathbb{S}_{rec}$: the non-reflected arrival of $\bar{G}_R^{(d)}$ in eq. 7 has simply twice the amplitude of $\bar{G}_R^{(d)}$ in eq. 2. Retrieving it is therefore no different than for eq. 2: one simply has to invert eq. (4), but without the factor 2 at the right-hand side and with the point-spread function and crosscorrelation function computed from the full wave fields. Figure 2b shows an example of a configuration for which reflecting boundaries in the reference medium are a convenient choice. We demonstrate the modified MDD formulation, considering a very simple 2D homogeneous acoustic medium and the configuration shown in Figure 3. Each source emits a Ricker wavelet with a central frequency of 10 Hz and unit maximum amplitude. Assuming a time dependence $e^{i\omega t}$, the frequency domain Green's function can be modeled using zeroth order Hankel functions of the second kind, i.e., $G(\mathbf{x}_A,\mathbf{x}_B,\omega) = (i/4)H_0^{(2)}(\omega|\mathbf{x}_A-\mathbf{x}_B|/c)$ for any $\mathbf{x}_A$ and $\mathbf{x}_B$. The velocity $c=\sqrt{K/\rho}$ is based on the bulk modulus and density of water, i.e., $K = 2.2\times10^9$ Pa and $\rho = 1000$ kg/m^3, respectively. The fact that we do not close the receiver boundary by placing receivers along $z=0$ and $z=2000$ does not violate the assumptions associated with eq. 7: the absence of sources at $z<0$ and $z>2000$ ensures that no energy propagates downward through $z=0$ and/or upward through $z=2000$. Radiation conditions therefore apply on those surfaces (Note that $z=0$ is not a free surface in this very simple example).

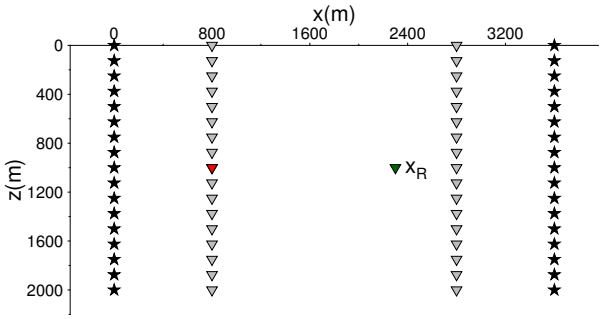

Figure 3: *Model setup for SI by MDD assuming a reflecting boundary in the reference state. Only every fifth source and receiver is depicted. The receiver acting as a virtual source is shown in red. Virtual source responses are reconstructed at the location of the green receiver.*

The regularly placed sources result in a (close to) uniform illumination pattern and hence the crosscorrelation function correctly estimates the dipole Green's function, which is shown in Figure 4a. The truncation at $z = 0$ and $z = 2000$ of the source array along $x = 0$, however, gives rise to a spurious arrival around $t = 0.85$ s (denoted by T1). MDD mostly corrects for the truncation effect, but cannot completely undo it. Figure 4b compares the crosscorrelation and MDD results for both negative and positive time. The peak at negative time disappears through the inversion, whereas additional peaks appear at positive time. One can, for example, clearly distinguish the first 'reflection' from the receiver boundary at $x = 3600$ (note the opposite polarity of the reflection). The peak denoted by T2 at about 2.5 s is a 'reflection' of the spurious arrival associated with the truncation at $z = 0$ and $z = 2000$ of the source array along $x = 3600$. Figure 4c shows the MDD reconstruction over a longer time range. By muting the (non-physical) reverberations of the response and spurious arrivals, one may extract the (improved) MDD response.

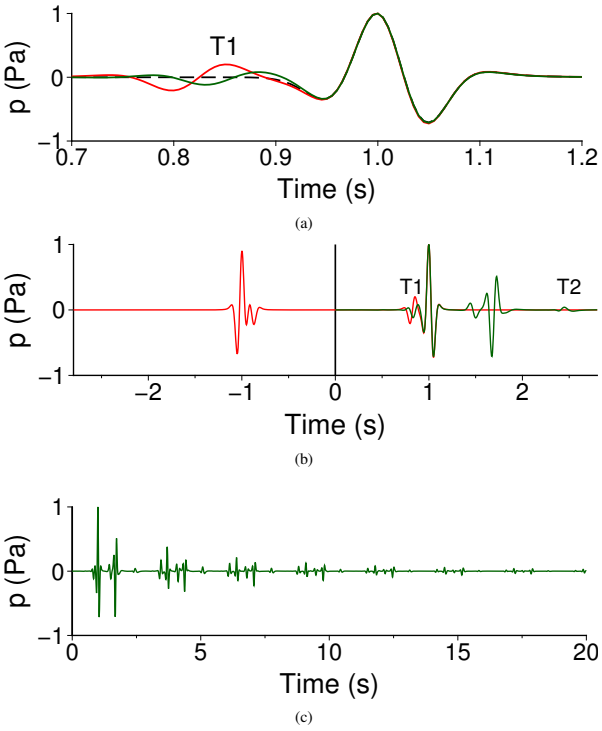

Figure 4: *Comparison of SI by crosscorrelation with SI by MDD. In (a) the responses reconstructed using SI by crosscorrelation (red line) and SI by MDD (green line) are compared to the directly modeled dipole Green's function (dashed black line). In (b) the crosscorrelation function is compared with the MDD result; (c) shows the reconstructed dipole Green's function over a longer time range. The reconstructed and directly modeled dipole Green's functions are convolved with the power spectrum of the sources. Amplitudes are normalized.*

SURFACE WAVE RETRIEVAL

The ambient seismic field is generally dominated by surface waves. In fact, it is often dominated by a single surface wave mode (Boschi et al., 2013; de Ridder and Biondi, 2013). Considering the particle displacement associated with a single component and surface wave mode, the elastodynamic convolution-type representation theorem can be written (van Dalen et al., 2014, 2015),

$$u(\mathbf{x}_R,\mathbf{x}_S,t) = 2\int_{\mathbb{S}_{rec}} \bar{G}_R^{(d)}(\mathbf{x}_R,\mathbf{x},t) * u^{(in)}(\mathbf{x},\mathbf{x}_S,t)\, d\mathbf{x}, \qquad (8)$$

where $u(\mathbf{x}_R,\mathbf{x}_S,t)$ represents the observed particle displacement at $\mathbf{x}_R$ and $u^{(in)}(\mathbf{x},\mathbf{x}_S,t)$ the observed particle displacement of the inward propagating wavefield along $\mathbb{S}_{rec}$; both due to a source at $\mathbf{x}_S$. The dipole Green's function $\bar{G}_R^{(d)}$ also represents particle displacement. Similar as for the acoustic case, we now assume a reflecting receiver boundary for the medium associated with $\bar{G}_R^{(d)}$. This implies,

$$u(\mathbf{x}_R,\mathbf{x}_S,t) = \oint_{\mathbb{S}_{rec}} \bar{G}_R^{(d)}(\mathbf{x}_R,\mathbf{x},t) * u(\mathbf{x},\mathbf{x}_S,t)\, d\mathbf{x}. \qquad (9)$$

Retrieving $\bar{G}_R^{(d)}$ involves SI by MDD, where the crosscorrelation and point-spread function are obtained in a similar way as in eqs. 5 and 6, respectively, but with the inward propagating wave field replaced by the complete wave field.

Anticipating future applications, we consider the configuration in Figure 5. The aperture of the closed receiver boundary is 10 km, resembling the aperture of contemporary ocean-bottom deployments (de Ridder and Biondi, 2013; Weemstra et al., 2013). Both phase velocity and (relative) amplitude of the sources are modeled using reasonable values for the Scholte waves traveling along the sea bed (de Ridder and Dellinger, 2011). In this example the medium is assumed to be homogeneous and dissipative (the Hankel functions are multiplied by an exponentially decaying term). Furthermore, crosscorrelations are summed over source locations. In practice one can simply average receiver-receiver crosscorrelations over sufficient time and/or time windows, provided the sources are uncorrelated (Wapenaar et al., 2011; de Ridder and Biondi, 2013). Our receiver boundary is illuminated by 300 randomly placed sources. The probability distribution governing the spatial placement of the the sources, however, is not uniform; for example, more sources are (expected to be) placed west of the receiver boundary than south.

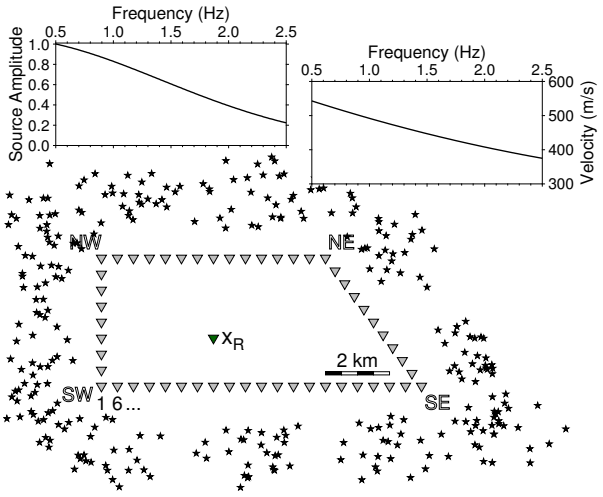

Figure 5: *Configuration for the simulation of single mode surface waves. Sources are irregularly distributed around the receiver array; all sources are depicted, only every fifth receiver is shown. The considered phase velocity and (relative) source amplitude are shown by the top right and top left inset, respectively.*

Figure 6 presents the virtual source response of every fifth boundary receiver. The responses reconstructed using SI by crosscorrelation and SI by MDD as well as the directly modeled (actual medium) responses are all normalized by the maximum amplitude on the 191^{st} trace. The relative amplitude differences between different virual-source responses are therefore maintained. We observe that the responses reconstructed using SI by crosscorrelation contain significantly more and stronger spurious arrivals. The responses obtained through SI by MDD are mostly free of energy prior to the non-reflected arrival and hence match the actual medium response (dashed black line) much better. The energy arriving later than the non-reflected response is due to 'reflections' from the receiver boundaries. By muting these 'non-physical' arrivals, one will be able to recover the response of the actual medium reconstructed through SI by MDD. In general, many strong heterogeneities in $\mathbb{V}$, i.e., in the actual medium, and/or crooked receiver boundaries may complicate the separation in time of the actual medium response and the later arrivals associated with the reflecting receiver boundary. For example, we observe in Figure 6 that close to the corners of the boundaries the reflected arrivals interfere with the non-reflected (actual medium) response (e.g., virtual source number 91).

CONCLUSIONS

We have derived an alternative formulation of the theory underlying seismic interferometry by MDD. Contrary to the conventional formulation, the new formulation allows deconvolution of the crosscorrelation function for irregularities in the illumination pattern using full wave fields rather than inward propagating wave fields. We therefore envisage the modified MDD formulation to hold significant promise in the application to ambient-noise surface wave data.

ACKNOWLEDGMENTS

This work is supported by the Netherlands Research Centre for Integrated Solid Earth Science (ISES). We thank Pablo David Garcia Lopez for his original comment, which led us to investigate the matter.

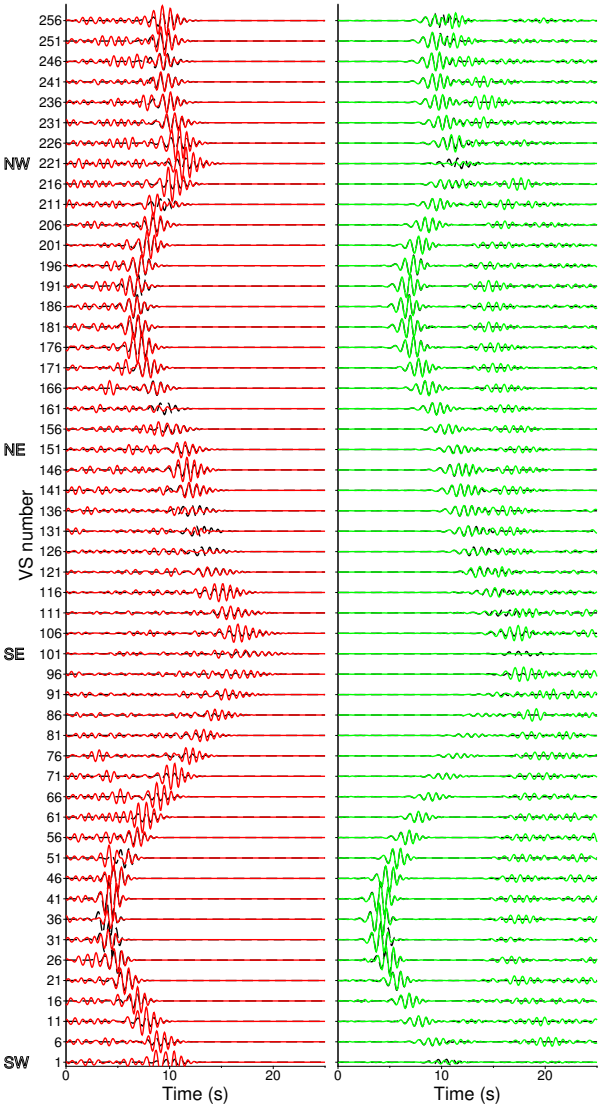

Figure 6: *Virtual source responses reconstructed through SI by crosscorrelation (red lines; left) and through SI by MDD (green lines; right) at the location of the green colored receiver in Figure 5. In both cases the reconstructed responses are compared to the directly modeled response (dashed black line). The reconstructed and directly modeled dipole Green's functions are convolved with the power spectrum of the sources. The values on the vertical axis refer to the boundary receiver numbers; the corners of the boundary are indicated for reference.*

REFERENCES

Bakulin, A., and R. Calvert, 2004, Virtual source: new method for imaging and 4D below complex overburden: SEG Technical Program Expanded Abstracts, **23**, 2477–2480.

Boschi, L., C. Weemstra, J. Verbeke, G. Ekstrom, A. Zunino, and D. Giardini, 2013, On measuring surface wave phase velocity from station-station cross-correlation of ambient signal: Geophysical Journal International, **192**, 346–358.

de Ridder, S., and J. Dellinger, 2011, Ambient seismic noise eikonal tomography for near-surface imaging at Valhall: The Leading Edge, **30**, 506–512.

de Ridder, S. A. L., and B. L. Biondi, 2013, Daily reservoir-scale subsurface monitoring using ambient seismic noise: Geophysical Research Letters, **40**, 2969–2974.

Froment, B., M. Campillo, P. Roux, P. Gouédard, A. Verdel, and R. L. Weaver, 2010, Estimation of the effect of nonisotropically distributed energy on the apparent arrival time in correlations: Geophysics, **75**, SA85–SA93.

Minato, S., T. Matsuoka, T. Tsuji, D. Draganov, J. Hunziker, and K. Wapenaar, 2011, Seismic interferometry using multidimensional deconvolution and crosscorrelation for crosswell sesimic reflection data without borehole sources: Geophysics, **76**, SA19–SA34.

Poletto, F., and C. Bellezza, 2012, Multidimensional deconvolution of seismic-interferometry Arctic data: SEG Technical Program Expanded Abstracts, **31**, 1–5.

van Dalen, K. N., T. D. Mikesell, E. N. Ruigrok, and K. Wapenaar, 2015, Retrieving surface waves from ambient seismic noise using seismic interferometry by multidimensional deconvolution: Journal of Geophysical Research: Solid Earth, **120**, 944–961.

van Dalen, K. N., K. Wapenaar, and D. F. Halliday, 2014, Surface wave retrieval in layered media using seismic interferometry by multidimensional deconvolution: Geophysical Journal International, **196**, 230–242.

van der Neut, J., 2012, Interferometric redatuming by multidimensional deconvolution: PhD thesis, Delft University of Technology.

Wapenaar, K., and J. Fokkema, 2006, Green's function representations for seismic interferometry: Geophysics, **71**, SI33–SI46.

Wapenaar, K., and J. van der Neut, 2010, A representation for Green's function retrieval by multidimensional deconvolution.: The Journal of the Acoustical Society of America, **128**, EL366–71.

Wapenaar, K., J. van der Neut, E. Ruigrok, D. Draganov, J. Hunziker, E. Slob, J. Thorbecke, and R. Snieder, 2011, Seismic interferometry by crosscorrelation and by multidimensional deconvolution: a systematic comparison: Geophysical Journal International, **185**, 1335–1364.

Weemstra, C., L. Boschi, A. Goertz, and B. Artman, 2013, Seismic attenuation from recordings of ambient noise: Geophysics, **78**, Q1–Q14.